Isotropic–nematic transition of long, thin, hard spherocylinders confined in a quasi-two-dimensional planar geometry

Marco Cosentino Lagomarsino[a] and Marileen Dogterom[a]
FOM Institute for Atomic and Molecular Physics (AMOLF), Kruislaan 407, 1098 SJ Amsterdam, The Netherlands

Marjolein Dijkstra[b]
Debye Institute, Soft Condensed Matter Physics, Utrecht University, Princetonplein 5, 3584 CC Utrecht, The Netherlands

(Received 7 March 2003; accepted 12 May 2003)

We present computer simulations of long, thin, hard spherocylinders in a narrow planar slit. We observe a transition from the isotropic to a nematic phase with quasi-long-range orientational order upon increasing the density. This phase transition is intrinsically two-dimensional and of the Kosterlitz–Thouless type. The effective two-dimensional density at which this transition occurs increases with plate separation. We qualitatively compare some of our results with experiments where microtubules are confined in a thin slit, which gave the original inspiration for this work.
© *2003 American Institute of Physics.* [DOI: 10.1063/1.1588994]

I. INTRODUCTION

Two-dimensional systems behave generically in a qualitatively distinct way from three-dimensional ones. In experiments, they are often not strictly confined to a mathematical surface, but also span a small region in the transverse dimension. A situation where two hard walls very close to each other confine the system occurs between the two extremes of bulk and two dimensions, and, for this reason, is interesting to analyze. We study the phase behavior of a system confined between two parallel planar plates separated by small distances as a function of the plate separation, and relate it to the corresponding strictly two-dimensional system. We address this question, using computer simulations, for the isotropic–nematic (I–N) transition of thin, hard spherocylinders. The inspiration for this problem comes from a biological system, cortical microtubules in plant cells, and by *in vitro* experiments on microtubules confined in thin samples. Microtubules are tubular polymers of the protein tubulin with an aspect ratio of a few hundreds. They are the stiffest polymers available to eukaryotic cells, with a persistence length of about three millimeters,[1] two orders of magnitude greater than their typical length. Using microtubules one can construct a good model system for the quasi-two-dimensional regime of (broadly polydisperse) hard rods. In this paper, we focus on the results of our simulations, while also commenting on the possible links to the experimental system.

It is known[2,3] that a system of hard needles or high (>9) aspect ratio disco-rectangles in two dimensions exhibits, similarly to the *xy* model, a nematic transition to quasi-long-range order of the Kosterlitz–Thouless kind.[4] The role of disclinations in this system has been investigated for different two-dimensional geometries.[5] In addition, density functional theory calculations show that the isotropic–nematic transition in two-dimensional dispersions of self-assembled or polydisperse needles is continuous.[6] A related problem is that of surface effects in the presence of a single wall.[7–9] Several theoretical and simulation studies were focused on fluids of hard rods in contact with hard walls. Chen and Cui performed density functional theory calculations for a fluid of hard, semiflexible polymers near a hard wall. They show a weakly first-order uniaxial to biaxial transition (signature of two-dimensional ordering in the plane defined by the wall) at a bulk density far below that of the bulk I–N transition.[10] They also observe the formation of a biaxial nematic film at the wall–isotropic fluid interface with the director parallel to the wall. The thickness of this film appears to diverge as bulk I–N coexistence is approached.[10] A surface-induced continuous transition from a uniaxial to a biaxial phase prior to complete wetting was also predicted by density functional theory of the Zwanzig model,[9,11,12] in which the orientations of the particles are restricted to three orthogonal directions, and confirmed by simulations for freely rotating spherocylinders.[9,13] Returning to the case of a fluid confined by two parallel hard walls, it was found by simulations of freely rotating spherocylinders[13] and by density functional theory calculations of the Zwanzig model[11] that the surface-induced uniaxial to biaxial transition is prior to a first-order capillary nematization transition at larger bulk densities, which terminates in a capillary critical point when the wall separation is about twice the length of the rods.

This paper is organized as follows: In Sec. II we present our model of hard spherocylinders confined between two parallel planar hard walls, and we introduce the quantities that are measured, namely, the nematic order parameter and the orientational correlation function. In Sec. III, we present the results and we discuss the polydisperse case and the qualitative agreement with the experimental system. Our main result is that similarly to the strictly two-dimensional

[a]Electronic mail: cosentino-lagomarsino@amolf.nl, dogterom@amolf.nl
[b]Electronic mail: m.dijkstra@phys.uu.nl

 © 2003 American Institute of Physics

Downloaded 14 Nov 2003 to 131.211.35.132. Redistribution subject to AIP license or copyright, see http://ojps.aip.org/jcpo/jcpcr.jsp

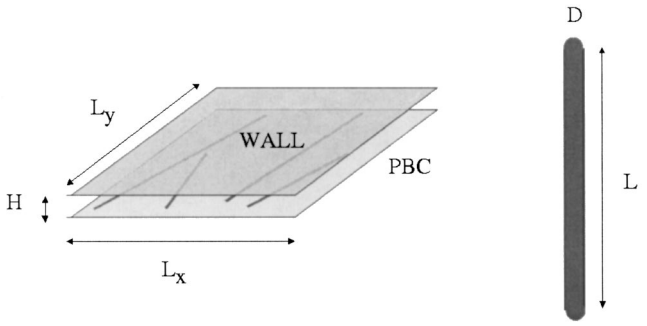

FIG. 1. A schematic picture of the system, which consists of a slit of thickness $h=H/D$, enclosed by two planar hard walls in the $x-y$ plane with dimensions $L_x \times L_y$. A particle (spherocylinder) is described by a cylinder of length L and diameter D capped by two hemispheres of the same diameter. Periodic boundary conditions are applied laterally.

system, there is no true transition to long-range order in the thermodynamic limit. A thickness-dependent transition to quasi-long-range orientational order of the Kosterlitz and Thouless kind is present instead.

II. A FLUID OF HARD SPHEROCYLINDERS CONFINED IN A QUASI-TWO-DIMENSIONAL PLANAR SLIT

We perform Monte Carlo simulations for a fluid of hard spherocylinders with a (mean) length-to-diameter ratio $L/D=320$, corresponding to microtubules of 8 μm in length and 25 nm in diameter, confined between two planar hard walls with an area of $L_x \times L_y$ in the $x-y$ plane at distance $h=H/D$ in the z direction (see Fig. 1). Periodic boundary conditions are employed in the x and y direction. The simulations are carried out in the canonical ensemble,[14] i.e., we fixed the number of particles N, the total volume $V=L_xL_yH$, and the temperature T. The slit width h varies from 1 to 120. We simulate both a system of monodisperse rods and a system of polydisperse rods with an exponential length distribution, which resembles closely the experiment with microtubules (see Sec. III). The simulations consist of about 2×10^6 Monte Carlo sweeps, where one sweep equals one attempted move per particle. Typically more than 10^5 Monte Carlo sweeps were allowed for equilibration. The number of particles N in a simulation is up to 5000, although typically lower than 2000.

We perform simulations for monodisperse spherocylinders for varying dimensionless densities

$$C=\frac{N}{V}(L+D)^2D,$$

where N is the number of particles, $V=L_xL_yH$ is the total volume, and $(L+D)^2D$ the maximum volume excluded by one particle. We measure the eigenvalues of the standard 3×3 nematic order-parameter tensor

$$Q_{\alpha\beta}=\left\langle \frac{1}{N}\sum_{i=1}^{N}\left(\frac{3}{2}u_\alpha^i u_\beta^i-\frac{\delta_{\alpha\beta}}{2}\right)\right\rangle,$$

where $\alpha,\beta=x,y,z$; u_α^i is the α component of the unit vector defining the orientation of particle i, and $\delta_{\alpha\beta}$ is Kronecker's delta. Diagonalizing $Q_{\alpha\beta}$ gives the orientational order parameters. As the typical cylindrical symmetry of the nematic state is broken *a priori* by the geometric constraints on the system, the most suitable order parameter Δ is proportional to the difference between the two highest eigenvalues of the average nematic tensor, normalized with a factor of 2/3 to make it lie in the interval [0, 1]. It is easy to realize that when $h=1$ this quantity reduces to the two-dimensional nematic order parameter,[2] and for larger h it can be identified with the biaxial order parameter.[9] In fact, for $h=1$, one of the three eigenvalues of Q will be $-1/2$ due to the geometric confinement, so that the submatrix defined by the other two eigenvalues will coincide with the exception of a constant factor with the two-dimensional nematic order parameter 2×2 tensor, and

$$\Delta\sim S=\left\langle \frac{1}{N}\sum_{i=1}^{N}\cos(2\theta_i)\right\rangle,$$

where θ_i is the planar smallest angle formed by the ith particle with the nematic director, and S is the two-dimensional orientational order parameter. We also examine the density and orientational order parameter Δ profiles along the axis orthogonal to the walls. These are measured using bins with a typical width of about D, accumulated over the sweeps in the simulation.[9] Last, we measure the orientational correlation function

$$g_2(r)=\langle(\cos(\theta(0)-\theta(r)))\rangle,$$

which describes the decay of the long wavelength fluctuations in the orientation.

III. RESULTS

We will first discuss the monodisperse case. The polydisperse system will be examined briefly, motivated by its relevance to experiments with microtubules.

A. Order parameter and size effects

Fixing the lateral size $L_x=L_y=L_{xy}$ of the system, we measure the order parameter Δ as a function of C. We find a transition to an ordered state for a density which depends slightly on h. In Fig. 2 we show typical snapshots of the fluid of spherocylinders for different densities of rods and a lateral view of the simulation box to illustrate its thickness. A transition from a uniaxial phase (in which the rods are randomly oriented in the xy plane) to a biaxial phase (the rods have a preferred orientation in the xy plane) is apparent from visual analysis of these pictures.

The order parameter and its profile along the z axis as a function of density are plotted for a few examples in Fig. 3. We define arbitrarily the apparent transition density C_{trans} as the density at the intersection of the tangents constructed on the low density part and the linearly increasing part of $\Delta(C)$ at fixed density (see Fig. 3).

The apparent phase transition from a uniaxial to biaxial phase, however, depends in all instances on the lateral size of the system. In fact, the order parameter drops with increasing size at fixed C, in a way that the apparent transition density

Downloaded 14 Nov 2003 to 131.211.35.132. Redistribution subject to AIP license or copyright, see http://ojps.aip.org/jcpo/jcpcr.jsp

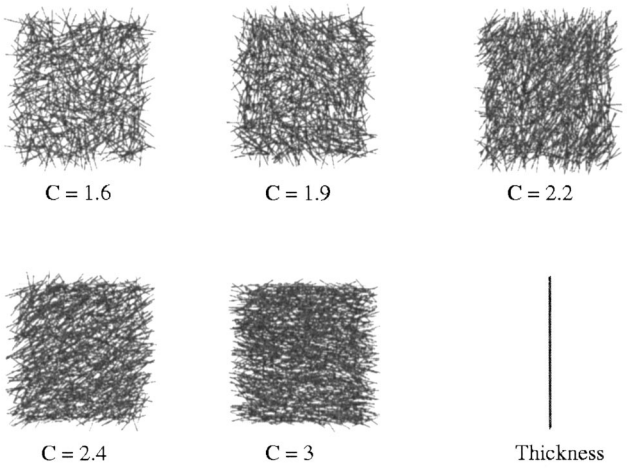

FIG. 2. Snapshots of the configuration of the system projected on the xy plane for different values of the dimensionless density $C=(N/V)(L+D)^2D$. Here, $h=20$, $L_{xy}=1400D$, N varies from 600 to 1150, and the equilibration time is 10^6 sweeps. The diameters of the rods are not drawn to scale.

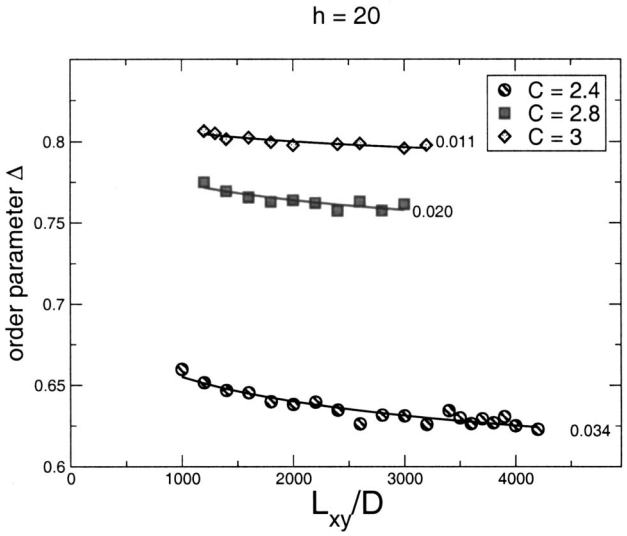

FIG. 4. Finite-size effects in the measurement of the order parameter Δ. The graph shows the decay of Δ for three dimensionless densities as a function of the lateral size L_{xy} when the vertical size $h=20$ is kept fixed. The numbers to the right of the curves are the exponent from power-law fits. The decay of the order parameter for increasing size causes a shift in the apparent transition.

increases. We measured this effect consistently for different transverse sizes ($h=5$, 20, 40, 60). In Fig. 4 we report an example for $h=20$.

This fact gives a hint that, as in the strictly two-dimensional system, there could be no true phase transition in the thermodynamic limit, but a transition to quasi-long-range order. To establish this, it is necessary to test whether the orientational correlation function shows an algebraic decay (see below).

For comparison with real finite-size systems it is interesting to look at the apparent transition density C_{trans}, at fixed lateral size L_{xy}, varying the small transverse size h. Two examples of the resulting phase diagrams are reported in Fig. 5. The transition density is roughly constant for thicknesses lower than $h=15$ [see Fig. 5(b)] and increases almost linearly for thicker boxes [see Fig. 5(a)].

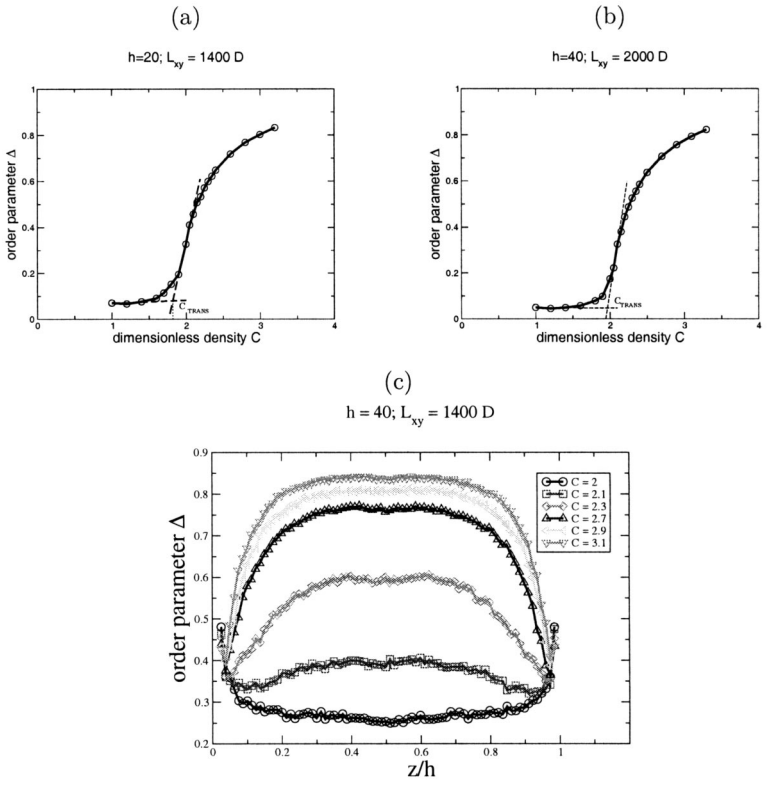

FIG. 3. (a) and (b) Order parameter Δ as a function of nondimensional density for $L_{xy}=1400D$. (a) $h=20$ (b) $h=40$. The transition density C_{trans} can be defined through the intersection of the tangents [dashed lines in (a) and (b)] constructed on the low density part and the linearly increasing part of the graphs. (c) z profile of the order parameter for $h=40$, $L_{xy}=1400D$, and increasing density.

Downloaded 14 Nov 2003 to 131.211.35.132. Redistribution subject to AIP license or copyright, see http://ojps.aip.org/jcpo/jcpcr.jsp

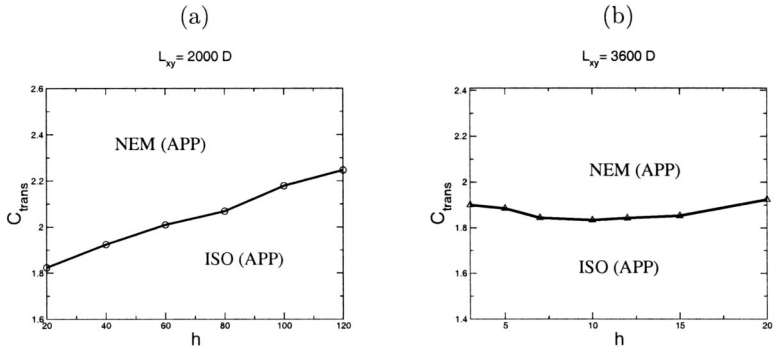

FIG. 5. Phase diagrams for the apparent nematic transition at fixed lateral size L_{xy}. The reduced uniaxial–biaxial transition density C_{trans} for different values of h. (a) Lateral size $L_{xy}=2000D$, thickness from $h=20$ up to $h=120$; the number of particles N for these runs is up to 7000. (b) Lateral size $L_{xy}=3600D$, thickness up to $h=20$, N up to 6000. The two critical lines in (a) and (b) do not connect continuously at $h=20$ because of the finite-size effects.

B. Correlation function

As we argued in the previous section, because of the finite-size effects (decrease of Δ with increasing size), little can be concluded about the nature of the phase transition, or even its existence based on the measurements of the order parameter. These finite-size effects, together with the presence of a phase transition to quasi-long-range order in the strictly two-dimensional system, make it sensible to investigate the decay of long wavelength orientational fluctuations. This is a delicate matter due to the very long relaxation times of these soft modes. We investigated the transition for integer values of h up to $h=10$, with a simulation box having a lateral size $L_{xy}=4000D$. Above this thickness, the number of particles was too high to achieve relaxation in reasonable times. In all these cases $g_2(r)$ showed a transition from exponential to power-law decay with increasing density. One example, for $h=6$, is plotted in Fig. 6. This transition does not depend on the size of the system, which just needs to be large enough so that the correlation of the modes is not affected by the periodic lateral boundary conditions.

From the above data, we can conclude that we are observing the same phase transition as in the two-dimensional system of needles, described by the Frank elastic free energy

$$F=\tfrac{1}{2}K\int \nabla\theta(\mathbf{r})d\mathbf{r}.$$

Therefore, we can set the transition density C_{trans}^{KS} when the exponent of g_2 crosses 1/4.[2] Going to the limiting case $h=1$, we can recover the fully two-dimensional system and compare the transition density with the one given in Ref. 2. We measure a $C_{\text{trans}}^{KS}(h=1)=6.5$ which we consider in good agreement with the 7.5 to 8 of Frenkel and Eppenga, considering the longer relaxation times we allow (5×10^5 sweeps for up to 2600 particles). This value can also be compared with the 5.3 found in Ref. 3 for disco-rectangles with $L/D=15$. The most interesting question, though, is how the transition density changes as a small lateral dimension is added. By a naive argument comparing the three-dimensional density C with the two-dimensional one $C_{2d}=(N/L_xL_y)(L+D)^2$, one would expect to see a transition density like $1/h$ so that the ''effective'' two-dimensional density is kept fixed. However, according to our data, shown in Fig. 7, this decay is slower than this power law. We can try to understand this by a qualitative argument based on the fact that this two-

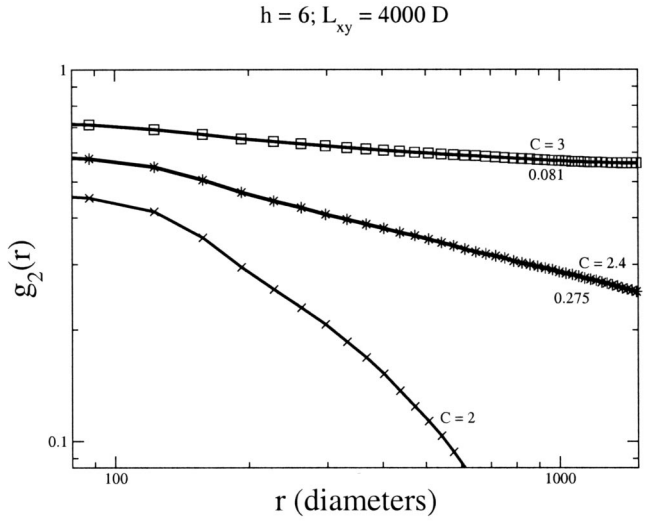

FIG. 6. Log–log plot of the orientational correlation function $g_2(r)$ for different values of the density, in the case $h=6$. For low density this quantity has exponential decay, which becomes algebraic with increasing C. The numbers next to the curves indicate the decay exponents from power-law fits. By convention, the transition is defined to be where the exponent of the correlation function crosses 1/4, in this instance around $C=2.4$.

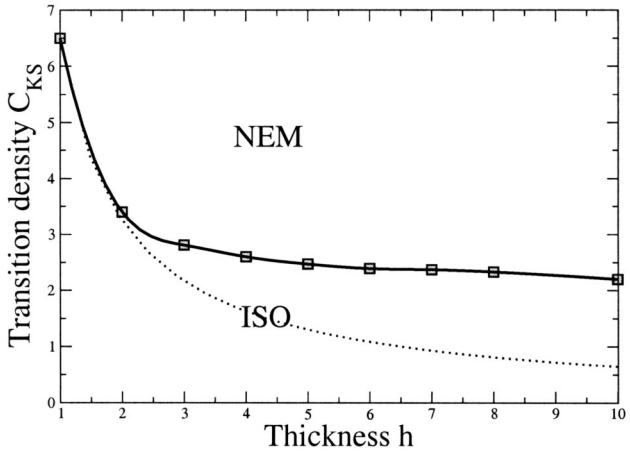

FIG. 7. Phase diagram for the nematic transition in quasi-two-dimensional geometry. The Kosterlitz–Thouless transition density C_{trans}^{KS} is plotted as a function of the system thickness h. Its decay is slower than the naively expected $1/h$ indicated by the dotted line.

Downloaded 14 Nov 2003 to 131.211.35.132. Redistribution subject to AIP license or copyright, see http://ojps.aip.org/jcpo/jcpcr.jsp

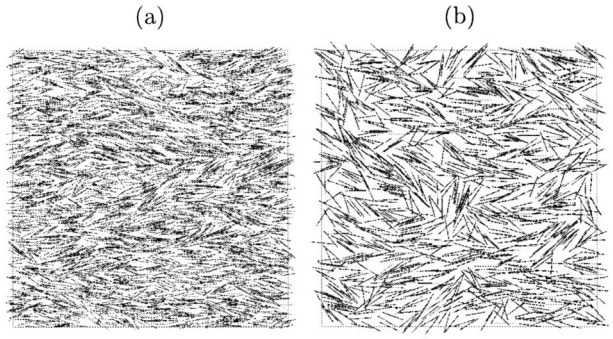

FIG. 8. Typical snapshots of configurations of two-dimensional nematic-like phases. The pictures are projections of the configurations on the *xy* plane. (a) 3074 particles in a slit with $h=1$, $L_{xy}=6000D$. The defects are noticeable in the picture. (b) 1150 particles in a slit with $h=3$, $L_{xy}=4000D$. Along with the defects, overlaps between projections of particles due to the transverse degrees of freedom are visible.

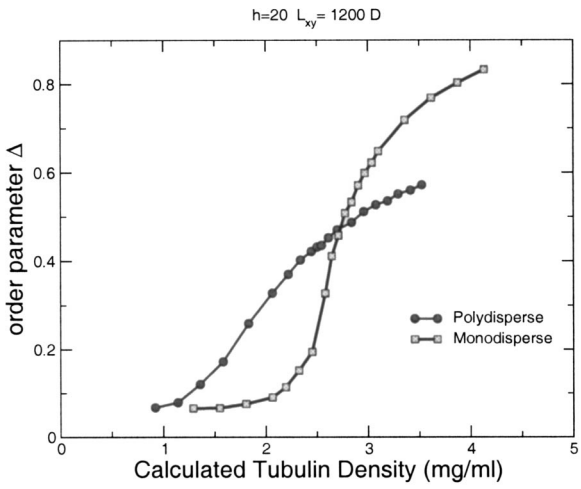

FIG. 9. Apparent transition predicted by the simulation for the experimental situation. The exponentially polydisperse case for a fixed size $L_{xy}=1200D$ is compared to the (simulated) monodisperse system with the same mean aspect ratio (320). The order parameter is computed in the usual way. The simulated system size $L_{xy}=1200D$ corresponds to a window of observation of 30×30 μm, which is comparable with that of a field of view of the microscope. In the *x* axis we plot the calculated (polymerized) tubulin density computed from the total length of the rods in the simulation box, using the fact that 1 μm of polymer contains ca. 1625 tubulin dimers, which in turn have a mass of about 100 kDa.

dimensional transition is mediated by defects. Adding a small transverse dimension, the liberty of effective overlaps given by the third degree of freedom makes it harder to form a disclination, so that a higher density than just $1/h$ times the two-dimensional one is required to achieve the transition. This fact is illustrated in Fig. 8, where we show two typical *xy* projections of the nematic states for $h=1$ and $h=3$. The configurations are qualitatively similar, but in the case $h=3$ many effective overlaps are noticeable.

C. Broadly polydisperse rods

We perform similar simulations for a system of polydisperse rods with an exponential length distribution. Our main motivation for doing this is to predict the experimental behavior of microtubules when they are confined in a region with a thickness that is very small compared to their (mean) length and very large compared to their diameter. The sample for such an experiment consists of a microscope coverslip patterned with 1 μm thick photoresist used to maintain a constant separation with the microscope slide (details will be published elsewhere).[16] In the experiment microtubules are broadly polydisperse, and typically show an exponential distribution in length with an average aspect ratio of a few hundreds. Their lengths do not vary in time due to stabilization with taxol.[15]

In the simulation of the polydisperse case, the apparent transition at fixed size is broader than the one observed for the monodisperse system (Fig. 9) and its onset is at lower densities, due to the effect of long rods. Nevertheless, the qualitative behavior of the system is the same, with size effects and power-law decay in the correlation function. By measuring the total length of the rods in one box, knowing that the length of a tubulin dimer is 8 nm and that each polymer is composed of 13 protofilaments, one can predict the concentration of polymerized tubulin needed to have the ordering transition at a fixed system size. The size of the system can be set as the field of view of the microscope, which is effectively the scale at which the experimental system is observed. With this identification, the apparent transition density, expressed in terms of tubulin concentration, falls in the experimentally accessible region of 2 to 5 mg/ml of (polymerized) tubulin.

Quantitative work on the experimental system is still in progress,[16] and involves a few complications. First, the density of polymerized tubulin cannot be implied directly from the amount flown in the sample, due to density variations in different locations of the sample and to uncertainties in the ratio of polymerized to unpolymerized protein. Second, the order parameter cannot be measured easily from image analysis because the individual rods cannot be distinguished from each other at high densities. However, the simulation results are qualitatively consistent with those observed experimentally (see Fig. 10 as an illustration), as the ordering transition can be observed for increasing microtubule densities within the range predicted by the simulation. Furthermore, in the experiment, microtubules are observed to order in ''patches'' of tens of microns in size, which is consistent with the absence of true long-range order predicted by the simulation.

IV. CONCLUSIONS AND PERSPECTIVES

We presented a Monte Carlo simulation of hard spherocylinders confined between two parallel walls at a small distance. This computation was intended to test the behavior of the nematic transition in a quasi-two-dimensional system. The main result is that a transition to long-range-order is absent in the thermodynamic limit. Instead, a Kosterlitz–Thouless-type transition is present, revealed by the algebraic decay of the orientational correlation function. This is in qualitative agreement with what is observed experimentally for a broadly polydisperse system of rod-like biological

Downloaded 14 Nov 2003 to 131.211.35.132. Redistribution subject to AIP license or copyright, see http://ojps.aip.org/jcpo/jcpcr.jsp

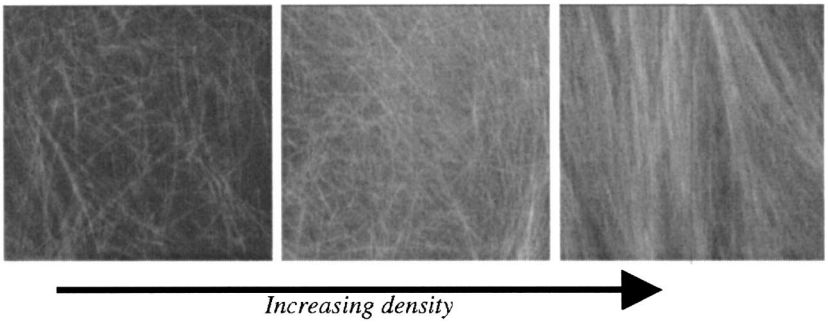

FIG. 10. Snapshots from the experiment. The microtubules, confined in 1 μm thick chambers, are imaged with fluorescence microscopy, the pictures show one field of view, sized 28×28 μm, obtained with a $100\times$ oil immersion lens. The concentration range of polymerized protein is estimated to be 1–4 mg/ml. The rods are observed to align for increasing densities on scales from 30 to 100 μm. On larger scales, patches of aligned rods with different orientation are noticeable. The local density of tubulin cannot be measured directly, but can be estimated comparatively from the average pixel intensity in the images after subtracting the background, provided that the settings of the CCD camera are fixed. In this figure, starting from the left, the second snapshot is approximately 1.5 times denser than the first, while the third is twice as dense as the second.

polymers (microtubules) and has some interesting general consequences. First of all, it indicates that a system with some small transverse third dimension will maintain the same qualitative behavior as a true two-dimensional one. Second, the slower decrease of the Kosterlitz–Thouless transition with increasing plate separations for the 2D-like isotropic–nematic transition indicates that there is an important role played by the transverse degree of freedom in the elimination of disclinations. Possible future work includes a quantitative exploration of the experimental system. It is also interesting to investigate in more detail the crossover between two- and three-dimensional behavior, exploring slit thicknesses that are comparable with the length of the rods. This kind of work would require using spherocylinders with a lower aspect ratio, to keep the number of particles, and therefore the computational cost, reasonably low. One possibility that we can hypothesize is that the Kosterlitz–Thouless transition in the strictly two-dimensional and quasi-two-dimensional system ends in the previously observed wall-induced uniaxial to biaxial transition[9] at larger plate separation, and is therefore not connected to capillary nematization (a transition from a biaxial to a condensed nematic phase), which terminates in a critical point at fixed plate separations.[11]

ACKNOWLEDGMENTS

We would like to thank Bela Mulder and Daan Frenkel for help and discussion. This work is part of the research program of the ''Stichting voor Fundamenteel Onderzoek der Materie (FOM),'' which is financially supported by the ''Nederlandse organisatie voor Wetenschappelijk Onderzoek (NWO).''

[1] F. Gittes, B. Mickey, J. Nettleton, and J. Howard, J. Cell Biol. **120**, 923 (1993).
[2] D. Frenkel and R. Eppenga, Phys. Rev. A **31**, 1776 (1985).
[3] M. A. Bates and D. Frenkel, J. Chem. Phys. **112**, 10034 (2000).
[4] J. M. Kosterlitz and D. Thouless, J. Phys. C **6**, 1181 (1973).
[5] J. Dzubiella, M. Schmidt, and H. Löwen, Phys. Rev. E **62**, 5081 (2000).
[6] P. van der Schoot, J. Chem. Phys. **106**, 2355 (1997).
[7] M. Schmidt and H. Löwen, Phys. Rev. Lett. **76**, 4552 (1996).
[8] A. Poniewierski, Phys. Rev. E **47**, 3396 (1993).
[9] R. van Roij, M. Dijkstra, and R. Evans, Europhys. Lett. **49**, 350 (2000).
[10] Z. Y. Chen and S. M. Cui, Phys. Rev. E **52**, 3876 (1995).
[11] R. van Roij, M. Dijkstra, and R. Evans, J. Chem. Phys. **113**, 7689 (2000).
[12] L. Harnau and S. Dietrich, Phys. Rev. E **66**, 051702 (2002).
[13] M. Dijkstra, R. van Roij, and R. Evans, Phys. Rev. E **63**, 051703 (2001).
[14] D. Frenkel and B. Smit, *Understanding Molecular Simulation* (Academic, San Diego, 2002), p. 111.
[15] A. Desai and M. Mitchison, Annu. Rev. Cell Dev. Biol. **13**, 83 (1997).
[16] M. Cosentino Lagomarsino and M. Dogterom (unpublished).

Downloaded 14 Nov 2003 to 131.211.35.132. Redistribution subject to AIP license or copyright, see http://ojps.aip.org/jcpo/jcpcr.jsp